Am J Transl Res 2020;12(7):3489-3500
www.ajtr.org /ISSN:1943-8141/AJTR0106268

Original Article

circ_BICD2 acts as a ceRNA to promote tumor progression and Warburg effect in oral squamous cell carcinoma by sponging miR-107 to enhance HK2

Lan-Sheng Zhu[1], Yan-Ling Wang[1], Rui Li[2], Xiao-Ting Xu[1], Kun-Yang Li[1], Chun-Ran Zuo[1]

[1]Department of Stomatology, Henan Province Hospital of TCM, Zhengzhou 450002, Henan, P. R. China; [2]Department of Stomatology, The First Affiliated Hospital of Zhengzhou University, Zhengzhou 450052, Henan, P. R. China

Received December 11, 2019; Accepted June 3, 2020; Epub July 15, 2020; Published July 30, 2020

Abstract: Numerous studies have proved that the Warburg effect serves a vital role involved in regulating the progression of malignant tumors. Previous studies confirmed that circRNAs act as a novel biomarker for diagnostic and therapeutic in various tumors. However, the functional role and mechanism of circ_BICD2 for the regulation of tumor growth and metastasis in oral squamous cell carcinoma (OSCC) via mediating the Warburg effect are largely unknown. In this study, we found that circ_BICD2 was upregulated in OSCC tumor tissues and cell lines. Inhibition of circ_BICD2 significantly decreased glycolysis, cell proliferation, migration and invasion of OSCC. Moreover, dual-luciferase reporter assay confirmed that circ_BICD2 directly targeted miR-107, as well as a targeted binding between miR-107 and HK2. Mechanistically, upregulation of miR-107 by circ_BICD2-silenced inhibited tumor growth by downregulating the HK2-mediated Warburg effect in OSCC. In conclusion, our findings suggested that circ_BICD2-deficient exerted anti-tumorigenesis and anti-glycolysis in OSCC by sponging miR-107 to downregulate HK2 expression, which provided a new potential therapeutic biomarker for OSCC clinical treatment.

Keywords: Oral squamous cell carcinoma, circ_BICD2, miR-107, HK2, Warburg effect

Introduction

Oral squamous cell carcinoma (OSCC) is one of the most destructive and fatal malignancies [1]. The incidence of OSCC has been increasing, with high lymphatic metastasis and distant metastasis [2]. There is no efficient tumor biomarker for OSCC diagnosis and treatment. Detecting the key factor in OSCC development and progression, and revealing the underlying mechanism could provide promising tumor biomarkers and candidate targets for OSCC diagnosis and treatment.

Previous studies found that dysregulation of circRNA was associated with the progression of various tumors [3, 4]. For example, Wang et al. reported that 1921 differentially expressed circRNAs in OSCC tumor tissues compared with the paired adjacent tissues [5]. Besides, circRNAs could regulate the expression of several oncogenes and tumor suppressor genes and activation or inactivation of the various signal pathways [6], thus modulating cell proliferation, migration, and invasion [7]. Moreover, increasing evidence confirmed that circRNAs might act as competing endogenous RNA (ceRNA) to regulate the progression of various tumors by sponging microRNAs (miRNAs) to mediate the expression of mRNA [8]. For instance, upregulation of circRNA_100533 suppressed OSCC cell proliferation, migration, and induced cell apoptosis by sponging miR-933 to upregulate GNAS expression [9]. Chen et al. circ_100290 serves as a ceRNA for miR-378a to promote OSCC cell proliferation and glycolysis [10]. Therefore, circRNAs could be promoting tumor biomarkers for tumor diagnosis and prognosis, and be a candidate target for tumor therapy. Recently, Zhao et al. showed that circ_0001874 (circ_BICD2) was highly expressed in the OSCC tumor tissues compared with the healthy control, and was correlated with TNM stage and tumor grade [11], but its detailed mechanisms in the progression of OSCC were still poorly understood.

Increasing evidence has confirmed that aerobic glycolysis has played an important regulatory

Table 1. Name and sequences of the primers

Name	Primer sequences
circ_BICD2	F: 5'-TTGGCTCTCCTGCTGTGC-3'
	R: 5'-GGTCATCCACAATCAGCCCA-3'
miR-107	F: 5'-AGCAGCATTGTACAGGG-3'
	R: 5'-GAATACCTCGGACCCTGC-3'
HK2	F: 5'-TGGCTGCCCACAAGATAATG-3'
	R: 5'-TCAATGTCGGCGCCTATTTC-3'
U6	F: 5'-CTCGCTTCGGCAGCACA-3'
	R: 5'-AACGCTTCACGAATTTGCGT-3'
β-actin	F: 5'-GAAATCGTGCGTGACATTAA-3'
	R: 5'-AAGGAAGGCTGGAAGAGTG-3'

F: Forward primer; R: Reverse primer.

role in the occurrence, development, migration, and invasion of various tumors [12]. In recent years, many studies have shown that targeting molecules inhibit glycolysis from achieving the purpose of inhibiting tumor progression [13, 14]. Interestingly, tumor cells exhibit an aberrant metabolism characterized by the high level of glycolysis, even in the presence of abundant oxygen. This phenomenon, known as the Warburg effect or aerobic glycolysis, facilitates tumor growth with elevated glucose uptake and lactate production [15]. Therefore, aerobic glycolysis may be a potential target for cancer therapy. Besides, circRNA targets miRNA to regulate tumor progression through mediating the Warburg effect, such as circ-FOXP1 promoted tumor progression and PKLR-mediated Warburg effect in gallbladder cancer by sponging miR-370 [16]. Ye et al. showed that knockdown of lncRNA FEZF1-AS1 suppressed tumor progression and Warburg effect via sponging miR-107 to decrease ZNF312B in pancreatic ductal adenocarcinoma [17]. Interestingly, online software called StarBase was predicted that miR-107 acts as a downstream target gene of circ_BICD2. However, the role and mechanism of circ_BICD2 regulated OSCC cell biological behavior and Warburg effect were remained obscure. The present study was aimed to uncover the underlying mechanisms of circ_BICD2 in the progression of OSCC *in vitro* and *in vivo*, and seek a new anticancer agent and target for the diagnosis and treatment of OSCC.

Materials and methods

Clinical samples

A total of 30 patients with OSCC were recruited in this study. None of whom had been previously treated with preoperative chemotherapy, radiotherapy, or other anticancer therapies prior to surgery. The clinical specimens (including tumor tissues and their paired adjacent tissues) were immediately snap-frozen in liquid nitrogen after surgical removal and after that transferred to a -70°C cryogenic refrigerator. This study was approved by the ethics committee of Zhengzhou University and all patients provided written consent. All the involved clinical experiments were conducted in accordance with the principle of the "Declaration of Helsinki".

Cell culture

The human OSCC cell lines (HSC-2, Tca8113, OSCC-15, SCC25 and Ca9-22), normal human oral epithelial cell lines (SG and NOK) and HEK-293T cells were purchased from the Shanghai Institutes for Biological Sciences of the Chinese Academy of Sciences (Shanghai, China). All cells were cultured in DMEM medium (HyClone, USA) containing 10% FBS (Capricorn, Germany) at 37°C in an incubator with a humidified atmosphere containing 5% CO_2.

Transfection

The pcDNA-circ_BICD2 (BICD2), circ_BICD2 shRNA (sh-BICD2), miR-107 inhibitor/mimic (miR-107/miR-inh), HK2 siRNA (si-HK2) and scrambled negative control were designed and constructed by Sangon Biotech (Shanghai, China). Both SCC25 and Ca9-22 cells were transfected with vectors all of the above, which were using the Lipofectamine 3000 kit (Invitrogen, USA) according to the manufacturer's instruction.

RT-qPCR

After the isolation of total RNA using the Trizol reagent purchased from Qiagen GmbH (Hilden, Germany). After that, the TaqMan Reverse Transcription Reagents (Applied Biosystems, USA) were employed to reverse transcription the total RNA to complementary DNA (cDNA). The SYBR Green PCR Master Mix (Takara, Japan) was next used to quantify the expression levels of targeted genes at transcriptional levels. The sequences of the involved primers were designed and listed in **Table 1**.

Western blot

The total proteins of tissues and cells were extracted using RIPA buffer added with Protease Inhibitor Cocktail (Cwbio, China), incubat-

ed on ice for 30 min, followed by centrifuged for 15 min at 14000 g. The proteins were separated by sodium dodecyl sulfate-polyacrylamide gel electrophoresis and then transferred to polyvinylidene difluoride (PVDF) membranes (Millipore, USA). After being blocked with 5% defatted milk for 1 h, the PVDF membranes were incubated with primary antibodies HK2 (1:1000, Abcam, USA), E-cadherin (1:1500, Abcam, USA), N-cadherin (1:1000, Abcam, USA), Vimentin (1:1000, Abcam, USA) and β-actin (1:2000, Abcam, USA) overnight at 4°C. The membranes were incubated with horseradish peroxidase-coupled secondary antibody (1: 3000, Abcam, USA) for 1 h at room temperature before being revealed using enhanced chemiluminescence reagent (Engreen, Beijing, China). The protein signals were detected using an Immobilon Western Chemiluminescent HRP Substrate kit (EMD Millipore, USA).

CCK-8 assay

CCK-8 assay was employed to explore cellular proliferation. After 24 h of incubation, transfected cells were treated with trypsin, collected, and seeded into 96-well plates with a density of 2×10^3 cells/well. CCK-8 assay was performed by adding 10 μL of CCK-8 solution (Shanghai Haling Biotechnology, Co., Ltd., Shanghai, China) into each well, after which the cells were incubated at 37°C for 2 h. The absorbance of the mixture in each well was read at 450 nm in a microplate reader (Bio-Rad Laboratories, Inc., Hercules, USA).

Colony formation assay

Both SCC25 and Ca9-22 cells were transfected with different vectors and cultured under the standard conditions. After that, the cells were diluted and seeded into 6-well plates at the density of 3000 cells per well for 14 days. The cells were then stained with 0.5% crystal violet (Beyotime, China) for 45 min. The colony number was counted using an inverted microscope produced by Thermo Fisher Scientific (USA).

Transwell migration and invasion assay

Forty-eight hours after transfection, both SCC25 and Ca9-22 cells were digested using trypsin, and the harvested cells were washed three with PBS. 2×10^4 cells were seeded on the surface of the Transwell upper chamber. Cell invasion assay should use the Transwell chamber covered with Matrigel (BD Biosciences, USA). Cells were incubated for 24 h, fixed with 4% paraformaldehyde. Then stain the cells with 0.1% crystal violet for 10 min. And PBS was utilized to clean the cells for three times. Finally, Select 5 random fields for further analysis.

Detection of Warburg effect in both OSCC cells

The effect of the circ_BICD2/miR-107/HK2 on Warburg effect of both OSCC cells was examined through detecting the levels of glucose uptake, lactate production and ATP generation using a commercial assay kit (Glucose uptake (#K924), Lactate production (#K627), ATP generation (#K345), BioVision, USA) according to the previous studies [18].

Dual-luciferase reporter gene system

The fragments of circ_BICD2 comprising wild-type (WT) and mutant (MUT) miR-107 binding sites were designed and synthesized by Shanghai GenePharma. The fragments were inserted into the pmirGLO dual-luciferase target expression vector (Promega Corporation, USA) to obtain the BICD2-WT and BICD2-MUT reporter plasmids. The HK2-WT and HK2-MUT reporter plasmids were generated in a similar manner. One night before transfection, the cells were seeded into 24-well plates at 60%-70% confluence. Either WT or MUT reporter plasmids were introduced into the cells in the presence of miR-107 mimic or mimic-NC. Forty-eight hours after transfection, the cells were collected, and their luciferase activity was measured using a dual-luciferase reporter assay system (Promega Corporation). Renilla luciferase activity was used to normalize the data.

RNA immunoprecipitation (RIP) assay

The RIP assay was conducted using the Magna RIP RNA-binding protein immunoprecipitation kit (Millipore, USA) according to the manufacturer's protocol. RIP was performed using SCC-25 cell lysate and either anti-AGO2 (ab32381, Abcam, UK) or Rabbit IgG (ab172730, Abcam, UK) as the antibody. Subsequently, RT-qPCR was performed to detect the expression of purified RNA.

Xenograft model

All experimental protocols involving animals were conducted following the guidelines of the Animal Protection Law of the People's Republic of China, 2009, and this study was performed

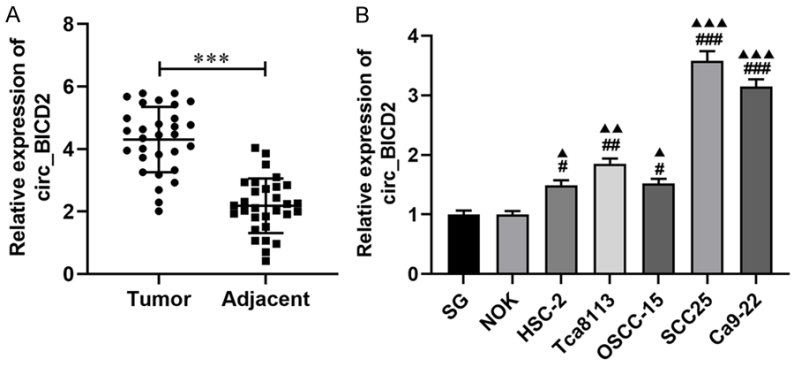

Figure 1. The expression of circ_BICD2 was overexpressed in OSCC tumor tissues and cell line. A. RT-qPCR revealed that the level of circ_BICD2 in OSCC tumor tissues and paired adjacent tissues. B. RT-qPCR was applied to detect the expression level of circ_BICD2 in human OSCC cell lines and normal human oral epithelial cell lines. Data are presented as means ± SD of three independent experiments. ***P<0.001, vs the paired adjacent tissues; #P<0.05, ##P<0.01, ###P<0.001, vs the SG cells; ▲P<0.05, ▲▲P<0.01, ▲▲▲P<0.001, vs the NOK cells.

Table 2. Associations between circ_BICD2 expression and clinicopathological characteristics

Clinical feature	Number	Expression of circ_BICD2		*P* value
		[a]High	Low	
	30	17 (56.67%)	13 (43.33%)	
Age (years)				0.880
≥60	18	10 (33.34%)	8 (26.66%)	
<60	12	7 (23.33%)	5 (16.67%)	
Sex				0.785
Male	17	10 (33.34%)	7 (23.33%)	
Female	13	7 (23.33%)	6 (20.00%)	
Tumor size (cm)				0.013
≥3	19	14 (46.66%)	5 (16.67%)	
<3	11	3 (10.00%)	8 (26.66%)	
TNM stage				0.035
I-II	12	4 (13.34%)	8 (26.66%)	
III-IV	18	13 (43.33%)	5 (16.67%)	
Lymph node metastasis				0.004
No	12	3 (10.00%)	9 (30.00%)	
Yes	18	14 (46.66%)	4 (13.34%)	

[a]The median of relative circ_BICD2 expression level is 4.3, so the number of high circ_BICD2 expression is 17 (>4.3).

under the approval of the Committee of Animal Research of the Zhengzhou University. A total of 20 female BALB/c nude mice (5 weeks old) were purchased from the Shanghai Experimental Animal Center of the Chinese Academy of Sciences (Shanghai, China) and maintained under a specific pathogen-free condition. The SCC25 cells stably transfected with circ_BICD2 shRNA (sh-BICD2) or sh-NC were subcutaneously injected into nude mice, which were subsequently categorized as sh-BICD2 (10 mice per group) and sh-NC mice, respectively. After injection, the size of the formed tumor xenografts was recorded every week, and their volume was analyzed using the formula volume (mm^3) = ½ × (Length × $Width^2$). All mice were sacrificed 4 weeks after implantation, and tumor xenografts were removed and weighed. In addition, total RNA and protein were extracted from tumor xenografts and examined using RT-qPCR and immunohistochemistry, respectively.

Statistical analysis

The data in this study are presented as mean ± standard deviation (SD) of 3 individual experiments and analyzed by a one-way ANOVA test, and the difference between the two groups was determined using the Student *t*-test, which was considered statistically significantly P<0.05, P< 0.01 or P<0.001. The Pearson Correlation analysis was performed using GraphPad Prism (Version 8.0; USA).

Results

Circ_BICD2 was upregulated in tumor tissues and cell lines in OSCC

The results turned out that circ_BICD2 was overexpressed in OSCC tumor tissues through using RT-qPCR (P<0.001, **Figure 1A**). By comparing clinicopathological characteristics (**Table 2**), the upregulated circ_BICD2 was closely related with tumor size (P<0.05), TNM stage (P<0.05) and lymph node metastasis (P<0.01).

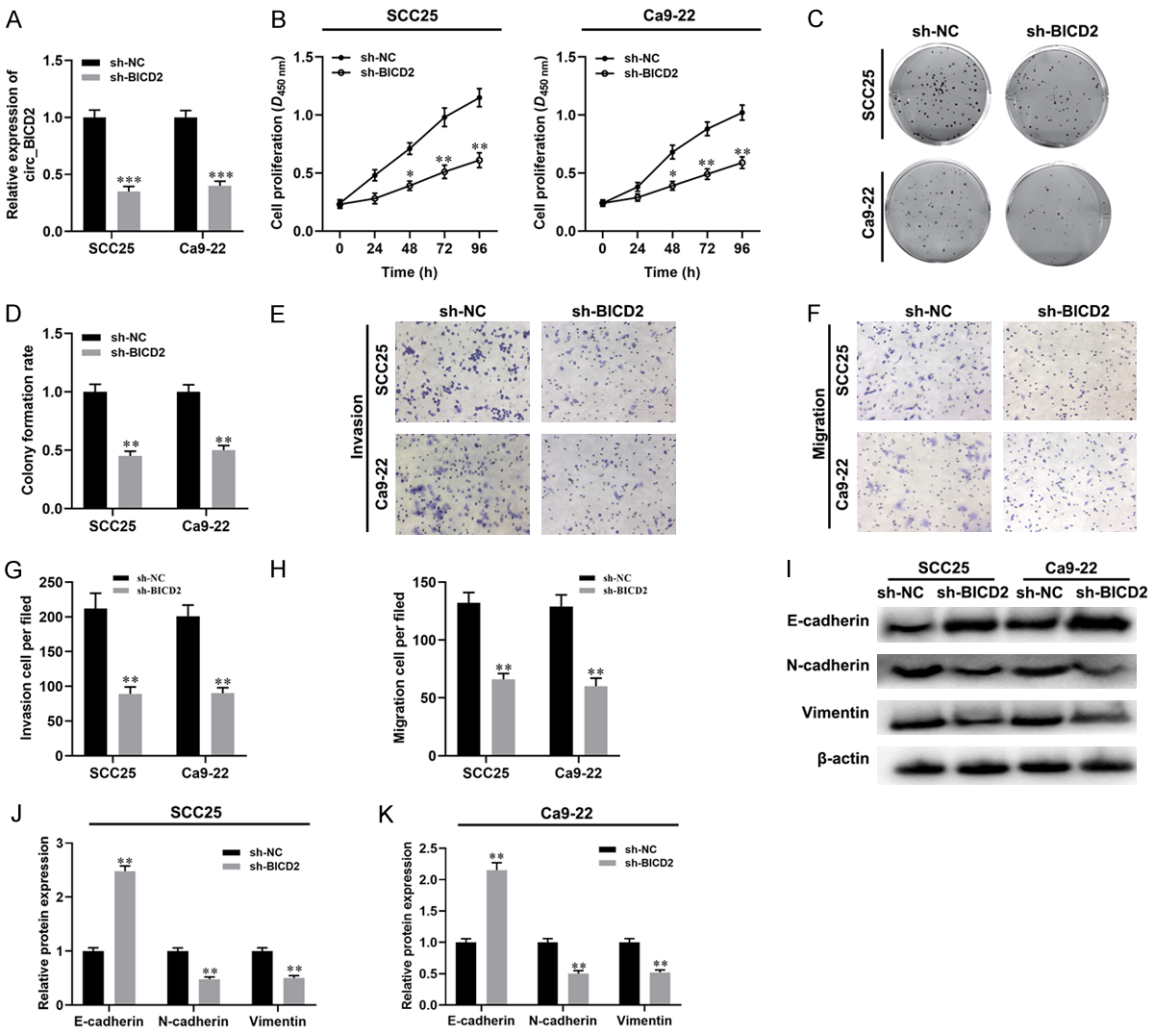

Figure 2. Knockdown of circ_BICD2 suppressed the malignant biological behavior of both OSCC cells. A. RT-qPCR was used to examine the expression of circ_BICD2 in both SCC25 and Ca9-22 cells when transfected with circ_BICD2 shRNA or shRNA control. B. CCK-8 assay was applied to evaluate the cell proliferation. C and D. Colony formation assay was used to evaluate the colony formation rate. E-H. The migration and invasion capacity of OSCC cells using Transwell assay. I-K. Western blot was performed to measure the protein levels of E-cadherin, N-cadherin and Vimentin. Data are presented as means ± SD of three independent experiments. *P<0.05, **P<0.01, ***P<0.001, vs the sh-NC group.

Moreover, the above results were also validated in cellular levels, which indicated that circ_BICD2 expressed highly in human OSCC cell lines compared with the normal oral epithelial cell lines (SG and NOK) (P<0.001, **Figure 1B**), especially both SCC25 and Ca9-22 cells (P< 0.001). Taken together, circ_BICD2 was markedly upregulated in OSCC tissues and cell lines.

Inhibition of circ_BICD2 inhibited malignant biological behavior of OSCC cells

To investigate the role circ_BICD2 in OSCC progression, we depleted circ_BICD2 in both SCC25 and Ca9-22 cells via transfecting with circ_BICD2 shRNA (P<0.001, **Figure 2A**). Besides, The CCK-8 assay and colony formation were employed to evaluate the effect of circ_BICD2-silenced on cell proliferation ability of both SCC25 and Ca9-22 cells and the results showed that knockdown of circ_BICD2 dramatically decreased cell proliferation (**Figure 2B-D**). Moreover, circ_BICD2-deficient SCC25 and Ca9-22 cells exhibited substantial decreases in migration (both P<0.01, **Figure 2E**, **2G**) and invasion (both P<0.01, **Figure 2F**, **2H**) compared with those observed in sh-NC-transfected cells. Similarly, western blot results showed

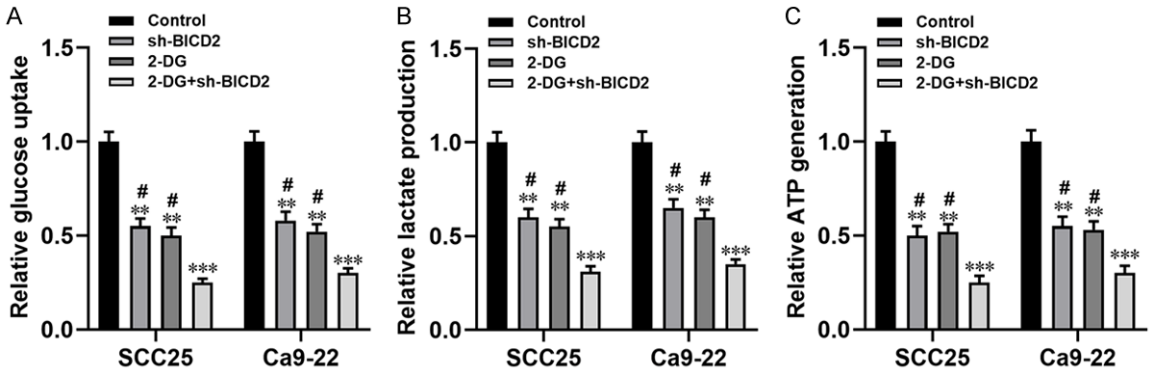

Figure 3. Inhibition of circ_BICD2 decreased the Warburg effect in both SCC25 and Ca9-22 cells. A. The glucose uptake colorimetric assay kit was used to detect the levels of glucose uptake in both SCC25 and Ca9-22 cells when transfected with circ_BICD2 shRNA or knockdown of circ_BICD2 plus 2-DG addition. B. The lactate colorimetric assay kit was applied to measure the level of lactate production. C. The ATP colorimetric assay kit was performed to examine the level of ATP generation in both SCC25 and Ca9-22 cells. Data are presented as means ± SD of three independent experiments. **P<0.01, ***P<0.001, vs the control group; $^{\#}$P<0.05, vs the 2-DG+sh-BICD2. sh-BICD2: circ_BICD2 shRNA; 2-DG: glycolytic inhibitor.

that knockdown of circ_BICD2 decreased the expression levels of N-cadherin and Vimentin (both P<0.01, **Figure 2I-K**), and enhanced the protein level of E-cadherin (both P<0.01). Taken together, inhibition of circ_BICD2 exerts anti-proliferation and anti-metastasis activities in OSCC cells.

Knockdown of circ_BICD2 decreased aerobic glycolysis in OSCC cells

Increasing evidence confirmed that circRNAs involved in the progression of various tumors by regulating the Warburg effect [10, 19]. Herein, we examined the effect of circ_BICD2 on glucose uptake, lactate production and ATP generation in both OSCC cells. Knockdown of circ_BICD2 significantly blocked the Warburg effect through downregulating the levels of glucose uptake, lactate production and ATP generation in both SCC25 and Ca9-22 cells (all P<0.01, **Figure 3**). Of note, the glycolytic inhibitor (2-DG) magnified the inhibitory effect of circ_BICD2-silenced on the Warburg effect in both SCC25 and Ca9-22 cells (P<0.001, **Figure 3**). In conclusion, the above results showed that knockdown of circ_BICD2 decreased glycolysis in OSCC cells.

Circ_BICD2 acts as a ceRNA to modulate HK2 expression via sponging miR-107

Previous studies confirmed that circRNAs regulated the development and progression of cancer through targeting miRNA [20]. In this study, we use an online software called StarBase to perform prediction and found that miR-107 may act as a downstream target of circ_BICD2 potentially, and the binding sites were shown in **Figure 4A**. As expected, the dual-luciferase reporter gene analysis results showed that overexpression of miR-107 decreased the luciferase activity of the BICD2-WT reporter compared with the NC group (P<0.01, **Figure 4C**). Besides, it was predicted that HK2 acted as a downstream target of miR-107 (**Figure 4B**). The dual-luciferase reporter gene system analysis found that the luciferase activity of the HK2-WT group was decreased by transfecting cells with miR-107 mimic (P<0.01, **Figure 4D**). Moreover, RIP analysis results showed that circ_BICD2, miR-107 and HK2 were enriched to AGO2 (P< 0.001, **Figure 4E**), upregulation of circ_BICD2 enhanced the enrichment of circ_BICD2 to AGO2 (P<0.001, **Figure 4F**), while decreased the enrichment of HK2 to AGO2 (P<0.01, **Figure 4F**), which indicated that circ_BICD2 acts as a ceRNA to regulate HK2 by competing binding to miR-107 in SCC25 cells. Similarly, knockdown of circ_BICD2 significantly decreased the protein level of HK2 in both SCC25 and Ca9-22 cells (both P<0.01, **Figure 4G-J**), but down-regulation of miR-107 reversed this effect (P<0.01). Furthermore, there was a negative correlation between the expression of miR-107 and circ_BICD2 (r=-0.631, P<0.001, **Figure 4K**) or HK2 (r=-0.783, P<0.001, **Figure 4L**) in 30 OSCC tumor tissues. Taken together, our data suggested that circ_BICD2 acts as a ceRNA to

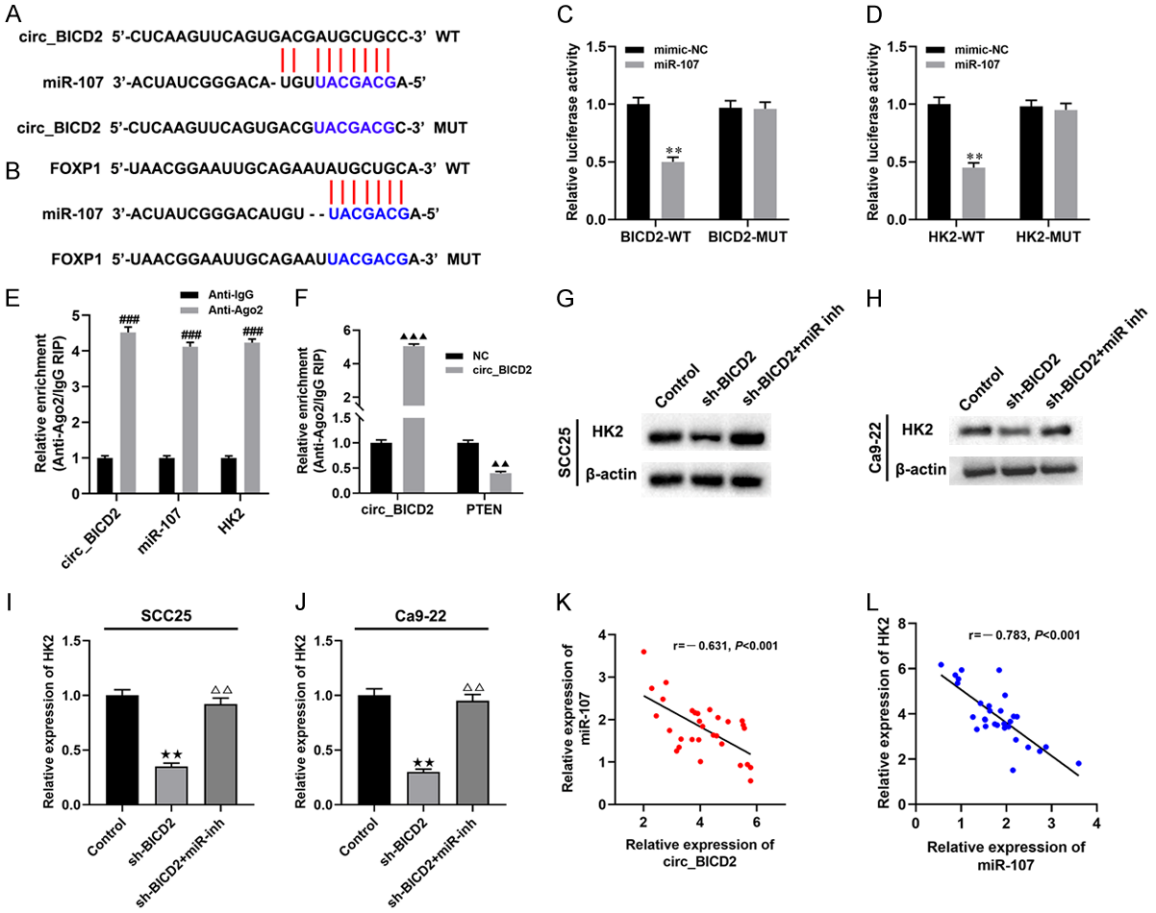

Figure 4. Circ_BICD2 acts as a ceRNA to modulate HK2 expression via sponging miR-107. A. Binding sites of miR-107 on circ_BICD2 were predicted. B. Binding sites of HK2 on miR-107 were predicted. C and D. Dual-luciferase reporter assay was employed to determine the regulation mechanisms of miR-107 and circ_BICD2 or HK2. E and F. RT-qPCR was applied to detect the expression of circ_BICD2, miR-107, and HK2 in AGO2 pellet. G-J. Western blot was applied to detect the protein level of HK2 in SCC25 cells. K and L. A negative correlation between the expression of miR-107 and circ_BICD2 or HK2 in OSCC tissues was observed using Pearson's correlation analysis. Data are presented as means ± SD of three independent experiments. **P<0.01, vs the mimic-NC group; $^{###}$P<0.001, vs Anti-IgG group; $^{▲▲}$P<0.01, $^{▲▲▲}$P<0.001, vs the NC group; $^{★★}$P<0.01, vs the control group; $^{△△}$P<0.01, vs the sh-BICD2 group.

modulate the expression of HK2 by sponging miR-107.

Circ_BICD2 regulates Warburg effect and biological behavior by sponging miR-107 to mediated HK2 expression in OSCC cells

To further explore whether circ_BICD2 mediates the Warburg effect and biological behavior of OSCC cells through regulating the miR-107/HK2 axis. Initially, both SCC25 and Ca9-22 cells transfected with HK2 siRNA, or co-transfected with miR-107 inhibitor or pcDNA-circ_BICD2 to change the expression level of HK2. The results showed that inhibition of HK2 downregulated the protein levels of HK2 in both SCC25 and Ca9-22 cells (both P<0.001, **Figure 5A**, **5B**), while co-transfected with miR-107 inhibitor or pcDNA-circ_BICD2 abolished this effect (both P<0.001). Moreover, we observed that suppression of the Warburg effect by inhibiting of HK2 in both SCC25 and Ca9-22 cells (all P<0.01, **Figure 5C-E**), but co-transfected miR-107 inhibitor or circ_BICD2 attenuated these effects (all P<0.01). In addition, we examined the effect of circ_BICD2 on the proliferation, invasion, and migration of both SCC25 and Ca9-22 cells via regulating the miR-107/HK2 axis. CCK-8 and colony formation assay showed that silencing of HK2 exerted anti-proliferation activity in both SCC25 and Ca9-22 cells (**Figure 6A-D**). However, co-transfected with miR-107

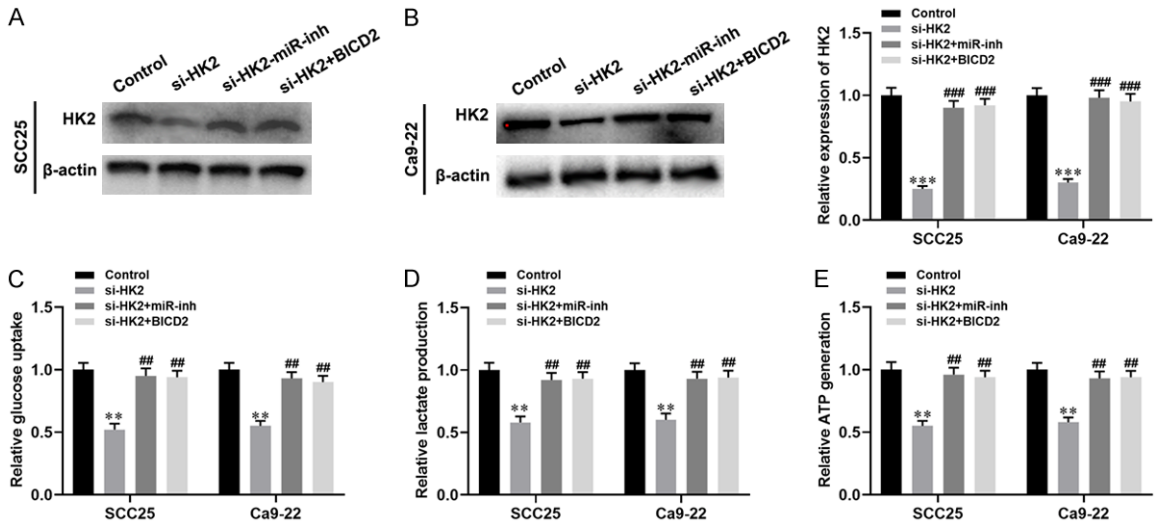

Figure 5. Circ_BICD2 regulates Warburg effect induced by HK2 vis sponging miR-107 in OSCC cells. A and B. Western blot was used to detect the expression of HK2 in both SCC25 and Ca9-22 cells. C. The glucose uptake colorimetric assay kit was used to detect the levels of glucose uptake in both SCC25 and Ca9-22 cells. D. The lactate colorimetric assay kit was applied to measure the level of lactate production. E. The ATP colorimetric assay kit was performed to examine the level of ATP generation in both SCC25 and Ca9-22 cells. Data are presented as means ± SD of three independent experiments. **P<0.01, ***P<0.001, vs the control group; $^{\#\#}$P<0.01, $^{\#\#\#}$P<0.001, vs the si-HK2 group.

inhibitor or pcDNA-circ_BICD2 reversed the effects of HK2-silenced on both OSCC cells. Furthermore, knockdown of HK2 inhibited the migration and invasion capacity of both SCC25 and Ca9-22 cells (both P<0.01, **Figure 6E-H**). However, co-transfected with miR-107 inhibitor or pcDNA-circ_BICD2 alleviated this effect (P< 0.01). In line with the results of cell migration and invasion, western blot results showed that inhibition of HK2 significantly suppressed the process of EMT in both SCC25 and Ca9-22 cells (**Figure 6I-L**). Taken together, our results suggested that knockdown of circ_BICD2 suppressed cell biological behavior and Warburg effect mediated by HK2 through sponging miR-107 in OSCC.

Knockdown of circ_BICD2 inhibited tumor growth and glucose uptake in vivo

In light of the effects of circ_BICD2 on OSCC cells in vitro, we further examined its effect on OSCC tumor growth, metastasis and Warburg effect in vivo. The nude mice in the sh-BICD2 group exhibited obviously hindered tumor growth in comparison with that observed in the sh-NC group (P < 0.01, **Figure 7A**). The weight of the tumor xenograft followed the same pattern, being lower in the sh-BICD2 group than that in the sh-NC group (P < 0.001, **Figure 7B**). Moreover, immunohistochemistry results demonstrated that knockdown of circ_BICD2 decreased the expression of Ki-67, Vimentin and HK2 in xenograft tumor tissues, as well as enhanced the expression of E-cadherin (**Figure 7C**). Furthermore, inhibition of circ_BICD2 decreased the level of glucose uptake compared with the control group (P<0.001, **Figure 7D**), as well as enhanced the expression of miR-107 (P<0.001, **Figure 7E**). In conclusion, our findings suggest that knockdown of circ_BICD2 may restrict OSCC progression by sponging miR-107 to decrease the HK2-mediated Warburg effect.

Discussion

The incidence of OSCC has been increasing, with high lymphatic metastasis and distant metastasis [21]. In this study, our findings confirmed that circ_BICD2 was overexpressed in OSCC tissues and cell lines. Knockdown of circ_BICD2 significantly decreased cell proliferation, migration, invasion, and glycolysis in OSCC. Furthermore, knockdown of circ_BICD2 acts as a ceRNA to inhibit tumor growth and metastasis by sponging miR-107 to decrease the HK2-mediated Warburg effect in OSCC.

Previous studies have proved that many cancers were characterized by abnormal expression of circRNAs, which played an essential role

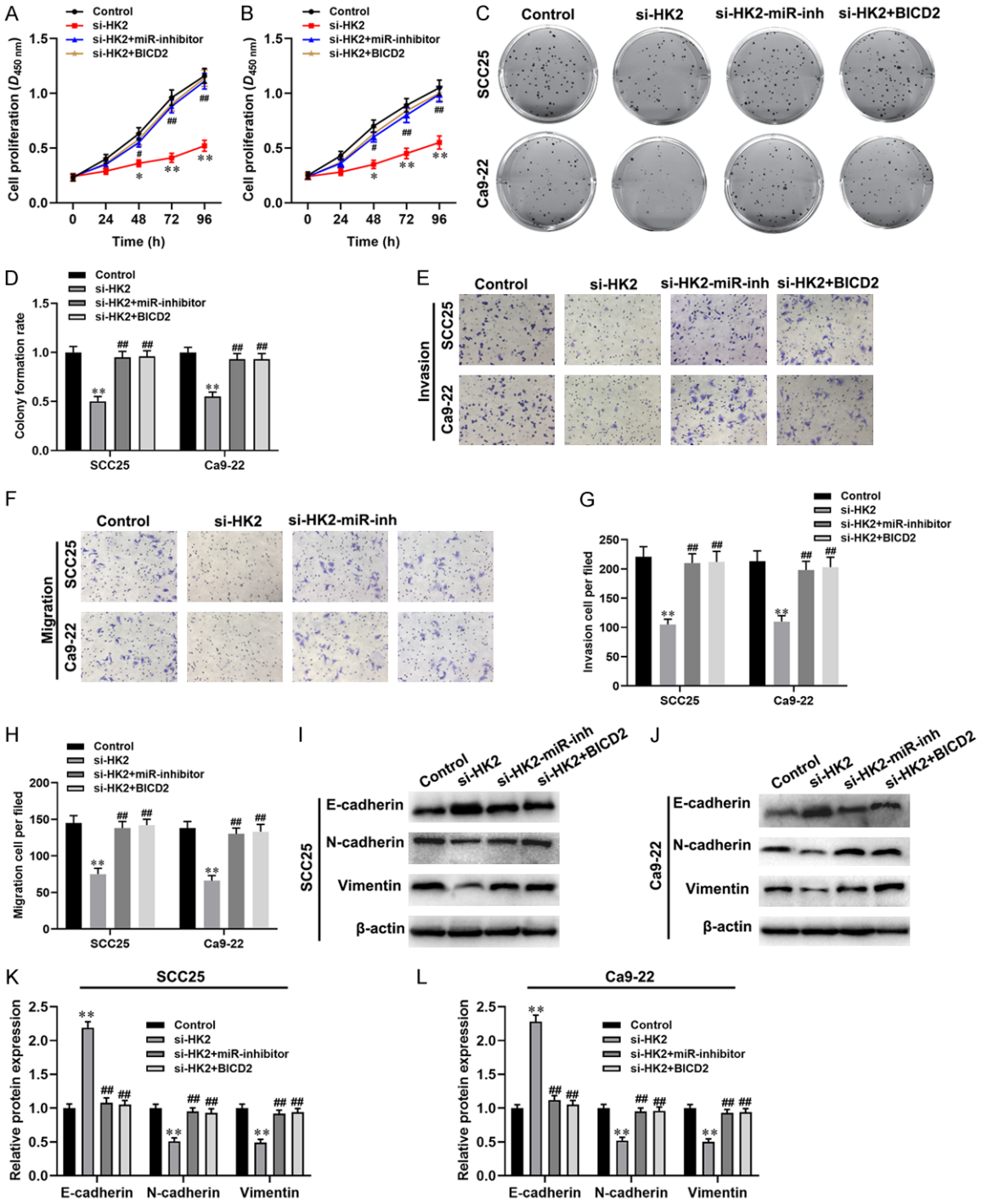

Figure 6. Circ_BICD2 knockdown inhibited the proliferation, migration and metastasis of both OSCC cell by competing binding to miR-107 to decrease HK2 expression. A and B. CCK-8 assay was applied to evaluate the cell proliferation. C and D. Colony formation assay was used to evaluate the colony formation rate. E-H. The migration and invasion capacity of OSCC cells using Transwell assay. I-L. Western blot was performed to measure the protein levels of E-cadherin, N-cadherin and Vimentin. Data are presented as means ± SD of three independent experiments. *P<0.05, **P<0.01, vs the control group; $^{\#}$P<0.05, $^{\#\#}$P<0.01, vs the si-HK2 group.

in the initiation and progression of carcinoma [22]. For example, low expression of circ_009-755 correlates with clinicopathology in OSCC [23]. Besides, circRNAs have emerged as important regulators of OSCC proliferation, migration, invasion, immune escape, and develop-

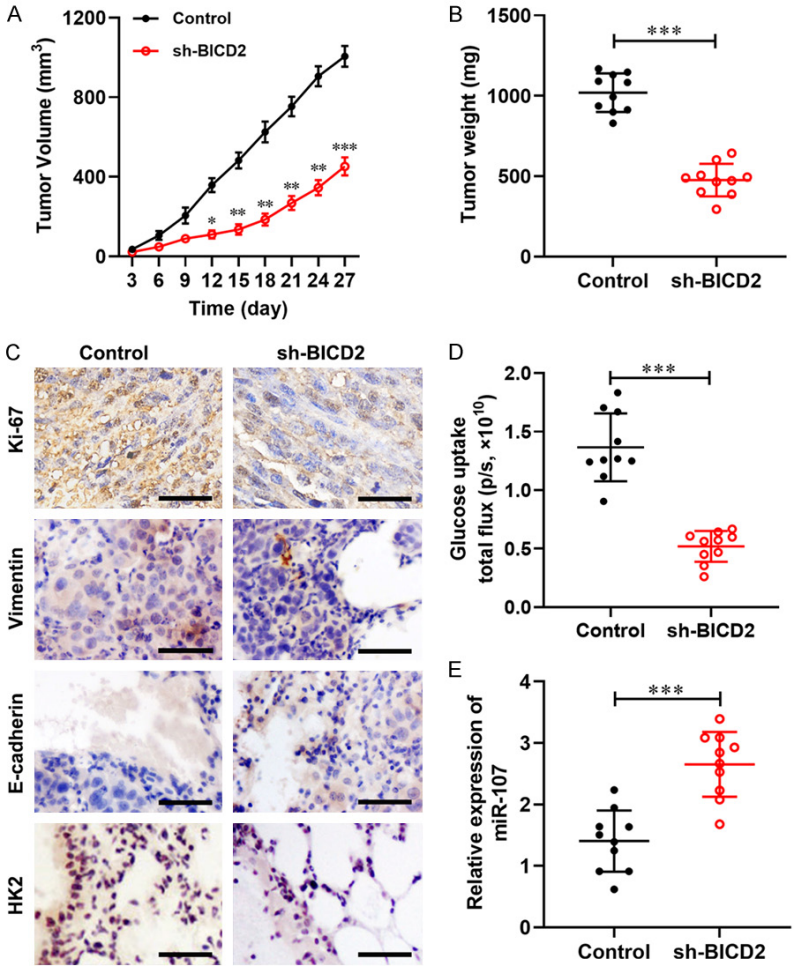

Figure 7. Knockdown of circ_BICD2 suppressed tumor growth, metastasis and Warburg effect in OSCC. A. The tumor volume curve of nude mice was analyzed. B. The tumor weight was measured. C. The expression of Ki-67, E-cadherin, Vimentin and HK2 were determined in tumor tissues using immunohistochemistry. D. The level of glucose uptake was examined. E. The expression of miR-23a-3p in the tumor tissues was measured using RT-qPCR. Data are presented as means ± SD of three independent experiments. *P<0.05, **P<0.01, ***P<0.001, vs the control group.

ment, as well as aerobic glycolysis and lipid metabolism. For example, circ_0005379 inhibited tumor growth and metastasis in OSCC [24]. Ouyang et al. showed that knockdown of circ_0109291 suppressed cell proliferation and migration of OSCC [25]. In line with previous studies, it is the first time to explore the role of circ_BICD2 in the proliferation and metastasis of OSCC cells. As expected, our studies found that circ_BICD2 was upregulated in tumor tissues and cell lines of OSCC, as well as inhibition of circ_BICD2 markedly suppressed OSCC cell proliferation, migration, and invasion. Furthermore, circRNAs can not only exhibit a vital role involved in the cellular biology and progression of OSCC, but also can affect the development of OSCC by interacting with different genes, for instance, Gao et al. found that circ-PKD2 inhibited tumor progression by sponging miR-204-3p to enhance APC2 expression in OSCC [20]. Chen et al. showed that circ_100290 serves as a ceRNA for miR-378a to promote cell proliferation by upregulating GLUT1-mediated Warburg effect in OSCC [10]. Similarly, our results found that inhibition of circ_BICD2 decreased tumor progression and Warburg effect via sponging miR-107 to decrease HK2 expression.

Cancer is a multi-step, multi-gene participation process [26]. Previous studies found that abnormal metabolism has become a major feature of tumor tissues that distinguishes it from normal tissues [27]. With continuous research, its role in the development of tumor was increasingly valued [28, 29]. Abnormal tumor metabolism not only provides energy for the rapid proliferation of tumor cells, synthetic raw materials, and a large number of reducing substances, but also affects tumor signal pathway conduction and gene expression, and then participates in the regulation of tumor cell growth, apoptosis resistance, migration and invasion attacks [30, 31]. In recent years, the abnormal metabolism of glucose in tumor cells has been the most in-depth metabolic research [12, 32]. Similarly, our data revealed that knockdown of circ_BICD2 decreased glucose uptake, lactate production, and ATP generation, as well as the addition of 2-DG augmented the inhibitory effect of circ_BICD2 suppression on glycolysis in OSCC. Moreover, miRNAs play a critical role in the biological and pathological processes through regulating the

Warburg effect in many human solid cancers, for example, miR-1244 inhibited cell proliferation and HK2-mediated glycolysis in ovarian cancer [33]. Xu et al. found that overexpression of miR-885-5p decreased the Warburg effect and cell proliferation via targeting HK2 in liver cancer [34]. In our present study, our study confirmed that miR-107 inhibited tumor growth and metastasis by decreasing the HK2-mediated Warburg effect in OSCC.

In summary, our study demonstrated that inhibition of circ_BICD2 significantly inhibited OSCC tumor growth and metastasis both *in vitro* and *in vivo*. Moreover, knockdown of circ_BICD2 notably decreased HK2 expression, which was a target gene of miR-107. Furthermore, silencing of circ_BICD2 suppressed cell proliferation, migration, invasion and Warburg effect through sponging miR-107 to downregulate HK2 expression. These findings suggested that the circ_BICD2/miR-107/HK2 axis may an effective biomarker for OSCC therapy through regulating cell metabolic.

Acknowledgements

This study was funded by the 2016 Henan Science and Technology Research Program Fund Project (No. 162102310183). No funding or other benefits related to the subject of this article were received from any commercial entity.

Disclosure of conflict of interest

None.

Address correspondence to: Dr. Lan-Sheng Zhu, Department of Stomatology, Henan Province Hospital of TCM, No.6 Dongfeng Road Jinshui District, Zhengzhou 450002, Henan Province, P. R. China. Tel: +86-0371-60970384; E-mail: lanshengzhu@163.com

References

[1] Tang JY, Hsi E, Huang YC, Hsu NC, Chu PY and Chai CY. High LC3 expression correlates with poor survival in patients with oral squamous cell carcinoma. Hum Pathol 2013; 44: 2558-2562.

[2] Shen ZS, Li JS, Chen WL and Fan S. The latest advancements in selective neck dissection for early stage oral squamous cell carcinoma. Curr Treat Options Oncol 2017; 18: 31-31.

[3] Qu S, Liu Z, Yang X, Zhou J, Yu H, Zhang R and Li H. The emerging functions and roles of circular RNAs in cancer. Cancer Lett 2018; 414: 301-309.

[4] Zhang Y, Liang W, Zhang P, Chen J, Qian H, Zhang X and Xu W. Circular RNAs: emerging cancer biomarkers and targets. J Exp Clin Cancer Res 2017; 36: 152-152.

[5] Wang YF, Li BW, Sun S, Li X, Su W, Wang ZH, Wang F, Zhang W and Yang HY. Circular RNA expression in oral squamous cell carcinoma. Front Oncol 2018; 8: 398-398.

[6] Su W, Wang Y, Wang F, Zhang B, Zhang H, Shen Y and Yang H. Circular RNA hsa_circ_0007059 indicates prognosis and influences malignant behavior via AKT/mTOR in oral squamous cell carcinoma. J Cell Physiol 2019; 234: 15156-15166.

[7] Su W, Sun S, Wang F, Shen Y and Yang H. Circular RNA hsa_circ_0055538 regulates the malignant biological behavior of oral squamous cell carcinoma through the p53/Bcl-2/caspase signaling pathway. J Transl Med 2019; 17: 76-76.

[8] Zhong Y, Du Y, Yang X, Mo Y, Fan C, Xiong F, Ren D, Ye X, Li C, Wang Y, Wei F, Guo C, Wu X, Li X, Li Y, Li G, Zeng Z and Xiong W. Circular RNAs function as ceRNAs to regulate and control human cancer progression. Mol Cancer 2018; 17: 79-79.

[9] Zhu X, Shao P, Tang Y, Shu M, Hu WW and Zhang Y. Hsa_circRNA_100533 regulates GNAS by sponging hsa_miR_933 to prevent oral squamous cell carcinoma. J Cell Biochem 2019; 120: 19159-19171.

[10] Chen X, Yu J, Tian H, Shan Z, Liu W, Pan Z and Ren J. Circle RNA hsa_circRNA_100290 serves as a ceRNA for miR-378a to regulate oral squamous cell carcinoma cells growth via glucose transporter-1 (GLUT1) and glycolysis. J Cell Physiol 2019; 234: 19130-19140.

[11] Zhao SY, Wang J, Ouyang SB, Huang ZK and Liao L. Salivary circular RNAs Hsa_Circ_0001874 and Hsa_Circ_0001971 as novel biomarkers for the diagnosis of oral squamous cell carcinoma. Cell Physiol Biochem 2018; 47: 2511-2521.

[12] Abdel-Wahab AF, Mahmoud W and Al-Harizy RM. Targeting glucose metabolism to suppress cancer progression: prospective of anti-glycolytic cancer therapy. Pharmacol Res 2019; 150: 104511-104511.

[13] Ganapathy-Kanniappan S and Geschwind JF. Tumor glycolysis as a target for cancer therapy: progress and prospects. Mol Cancer 2013; 12: 152-152.

[14] Gill KS, Fernandes P, O'Donovan TR, McKenna SL, Doddakula KK, Power DG, Soden DM and Forde PF. Glycolysis inhibition as a cancer

treatment and its role in an anti-tumour immune response. Biochim Biophys Acta 2016; 1866: 87-105.
[15] Lu J, Tan M and Cai Q. The Warburg effect in tumor progression: mitochondrial oxidative metabolism as an anti-metastasis mechanism. Cancer Lett 2015; 356: 156-164.
[16] Wang S, Zhang Y, Cai Q, Ma M, Jin LY, Weng M, Zhou D, Tang Z, Wang JD and Quan Z. Circular RNA FOXP1 promotes tumor progression and Warburg effect in gallbladder cancer by regulating PKLR expression. Mol Cancer 2019; 18: 145-145.
[17] Ye H, Zhou Q, Zheng S, Li G, Lin Q, Ye L, Wang Y, Wei L, Zhao X, Li W, Fu Z, Liu Y, Li Z and Chen R. FEZF1-AS1/miR-107/ZNF312B axis facilitates progression and Warburg effect in pancreatic ductal adenocarcinoma. Cell Death Dis 2018; 9: 34-34.
[18] Zheng J, Luo J, Zeng H, Guo L and Shao G. ^{125}I suppressed the Warburg effect viaregulating miR-338/PFKL axis in hepatocellular carcinoma. Biomed Pharmacother 2019; 119: 109402-109402.
[19] Yu T, Wang Y, Fan Y, Fang N, Wang T, Xu T and Shu Y. CircRNAs in cancer metabolism: a review. J Hematol Oncol 2019; 12: 90-90.
[20] Gao L, Zhao C, Li S, Dou Z, Wang Q, Liu J, Ren W and Zhi K. circ-PKD2 inhibits carcinogenesis via the miR-204-3p/APC2 axis in oral squamous cell carcinoma. Mol Carcinog 2019; 58: 1783-1794.
[21] Miguel AFP, Mello FW, Melo G and Rivero ERC. Association between immunohistochemical expression of matrix metalloproteinases and metastasis in oral squamous cell carcinoma: systematic review and meta-analysis. Head Neck 2019; 42: 569-584.
[22] Deng W, Peng W, Wang T, Chen J, Qiu X, Fu L and Zhu S. Microarray profile of circular RNAs identifies hsa_circRNA_102459 and hsa_circRNA_043621 as important regulators in oral squamous cell carcinoma. Oncol Rep 2019; 42: 2738-2749.
[23] Wang Z, Tang J, Wang Y, Sun S, Chen Y, Shen Y and Yang HY. Circular RNA hsa_circ_009755 downregulation correlates with clinicopathology in oral squamous cell carcinoma. Onco Targets Ther 2019; 12: 4025-4031.
[24] Su W, Wang Y, Wang F, Sun S, Li M, Shen Y and Yang H. Hsa_circ_0005379 regulates malignant behavior of oral squamous cell carcinoma through the EGFR pathway. BMC Cancer 2019; 19: 400-400.
[25] Ouyang SB, Wang J, Zhao SY, Zhang XH and Liao L. CircRNA_0109291 regulates cell growth and migration in oral squamous cell carcinoma and its clinical significance. Iran J Basic Med Sci 2018; 21: 1186-1191.
[26] Bhardwaj A, Bahl C, Sharma S, Singh N and Behera D. Interactive potential of genetic polymorphism in xenobiotic metabolising and DNA repair genes for predicting lung cancer predisposition and overall survival in North Indians. Mutat Res Genet Toxicol Environ Mutagen 2018; 826: 15-24.
[27] Fan T, Sun G, Sun X, Zhao L, Zhong R and Peng Y. Tumor energy metabolism and potential of 3-bromopyruvate as an inhibitor of aerobic glycolysis: implications in tumor treatment. Cancers (Basel) 2019; 11: 317.
[28] San-Millán I and Brooks GA. Reexamining cancer metabolism: lactate production for carcinogenesis could be the purpose and explanation of the Warburg Effect. Carcinogenesis 2017; 38: 119-133.
[29] Schwartz L, Supuran CT and Alfarouk KO. The warburg effect and the hallmarks of cancer. Anticancer Agents Med Chem 2017; 17: 164-170.
[30] Luo P, Zhang C, Liao F, Chen L, Liu Z, Long L, Jiang Z, Wang Y, Wang Z, Liu Z, Miao H and Shi C. Transcriptional positive cofactor 4 promotes breast cancer proliferation and metastasis through c-Myc mediated Warburg effect. Cell Commun Signal 2019; 17: 36-36.
[31] Li Z, Liu J, Que L and Tang X. The immunoregulatory protein B7-H3 promotes aerobic glycolysis in oral squamous carcinoma via PI3K/Akt/mTOR pathway. J Cancer 2019; 10: 5770-5784.
[32] de la Cruz-López KG, Castro-Muñoz LJ, Reyes-Hernández DO, García-Carrancá A and Manzo-Merino J. Lactate in the regulation of tumor microenvironment and therapeutic approaches. Front Oncol 2019; 9: 1143-1143.
[33] He Y, Chen X, Yu Y, Li J, Hu Q, Xue C, Chen J, Shen S, Luo Y, Ren F, Li C, Bao J, Yan J, Qian G, Ren Z, Sun R and Cui G. LDHA is a direct target of miR-30d-5p and contributes to aggressive progression of gallbladder carcinoma. Mol Carcinog 2018; 57: 772-783.
[34] Xu F, Yan JJ, Gan Y, Chang Y, Wang HL, He XX and Zhao Q. miR-885-5p negatively regulates warburg effect by silencing hexokinase 2 in liver cancer. Mol Ther Nucleic Acids 2019; 18: 308-319.